Beamforming MIMO array antenna for 5G-millimeter-wave application

Mantar Singh Mandloi
Shri G. S. Institute of Technology and Science
Parul Gupta
Shri G. S. Institute of Technology and Science
Ajay Parmar
Shri G. S. Institute of Technology and Science
Priyanshi Malviya
M. I. T. S., Gwalior, M.P.
Leeladhar Malviya (ldmalviya@gmail.com)
Shri G. S. Institute of Technology and Science https://orcid.org/0000-0002-7342-4766

Research Article

Keywords: MIMO, Beamforming, mm-Wave, ECC, TARC

Posted Date: June 3rd, 2022

DOI: https://doi.org/10.21203/rs.3.rs-1698818/v1

Beamforming MIMO array antenna for 5G-millimeter-wave application

Mantar Singh Mandloi[1†], Parul Gupta[2†], Ajay Parmar[3†], Priyanshi Malviya[4†] and Leeladhar Malviya[5*†]

[1]Electronics and Telecommunication, Shri G. S. Institute of Technology and Science, 23, Park Road, Indore, 452003, M.P., India.

[2]Electronics and Telecommunication, Shri G. S. Institute of Technology and Science, 23, Park Road, Indore, 452003, M.P., India.

[3]Electronics and Telecommunication, Shri G. S. Institute of Technology and Science, 23, Park Road, Indore, 452003, M.P., India.

[4]Electronics and Telecommunication, Madhav Institute of Technology and Science, Racecourse RD, Gwalior, 474005, M.P., India.

[5*]Electronics and Telecommunication, Shri G. S. Institute of Technology and Science, 23, Park Road, Indore, 452003, M.P., India.

*Corresponding author(s). E-mail(s): ldmalviya@gmail.com;
Contributing authors: mantar.mandloi@gmail.com; guptaparul1995@gmail.com; eng.ajayparmar@gmail.com; priyanshimalviya3@gmail.com;
†These authors contributed equally to this work.

Abstract

This paper presents low mutual coupling multiple input-multiple output (MIMO) array antenna for millimetre-wave (mmw) application. The MIMO-array beamforming antenna with 2:1 VSWR band is proposed for 28.0 GHz and covers 27.04 - 28.35 GHz frequency band, which is suitable for mm-wave n261 5G-band which cover the frequency range

from 27.5 - 28.35 GHz. It consists of 2×12 antenna array elements and the prototype is designed on low loss Rogers Duroid 5880 substrate of size 51.45×36.87 $\boldsymbol{mm^2}$. The beamforming MIMO antenna covers $\pm\mathbf{20^0}$ main lobe directions. The mutual coupling at the MIMO-array ports is less than 28.0 dB. The radiation efficiency and the gain in the presented band are more than 93.0% and more than 13.99 dBi. The ECC in the presented frequency band is $\leq \mathbf{10^{-4}}$, which is one of the advantages of the proposed design. The design covers indoor and outdoor Gaussian applications, and has 1.31 GHz TARC active bandwidth. It has 4.65% simulated and 4.73% measured fractional bandwidths.

Keywords: MIMO, Beamforming, mm-Wave, ECC, TARC

1 Introduction

Due to the tremendous increase in the high speed data rate, wireless communication may requires 1000 times more capacity in the future. In order to meet this exponentially demand, the fifth generation of wireless technologies are currently being developed for the millimetre-wave (mmw) communications, waveforms, multiple access, massive MIMO with beam-steering and dense networks. Antenna is the most primary constituents for the successful deployment of the wireless communication. MIMO uses spatial multiplexing where each data stream can be beam-formed to increase throughput. It is based on the principle that when the received signal quality is high, it is better to receive multiple streams of data with reduced power per stream than one stream with full power, as is done by single-input-single-output (SISO). Using non-line-of-sight (NLOS) communication, MIMO solves many drawbacks of SISO. Fifth generation of mobile networks are expected to provide very high connectivity speeds for uplink and downlink (upto 10 Gbps and more), reduction in per-bit-cost, low power consumption, larger data distribution, and intended/wide coverage for existing networking standards and allows integration of artificially intelligent (AI) devices, human-to-human communications, indoor hotspot (IH), dense urban (DU), and rural connectivity [1][2].

5G technology is expected to deliver the high data rate with low latency. The frequency band n261 27.5 - 28.35 GHz mmw have numerous advantage as it offers high resolution, data transfer at high speed, cost effectives and increased security making the mm-wave band an ideal candidature for 5G Technology. It is also depicted that most of the countries are considering the 27/28 GHz band for mmw 5G communication. Beamforming is the technique to guide the main lobe radiation beam in the desired directions at the transmitters and receivers with the help of MIMO/array elements, nullifying the undesired for spatial selectivity. Beamforming in present scenario is the most deserving candidate in RADAR, seismology, biomedical, SONAR etc. The

arrays, MIMO and Beamforming technologies are considered to be the key enablers for 5G mm-wave communication [3][4][5].

Varieties of antennas are available in literature for 5G applications. A multi-band (2.23 - 2.64 GHz and 3.26 - 3.70 GHz), multi-standard MIMO antenna for WLAN and Wi-MAX standards [6], a 4-port MIMO antenna with polarisation diversity technique for 1.68 - 2.24 GHz [7], an offset quad element multi-band (2.24 - 2.64 GHz and 3.41 - 3.69 GHz) planar MIMO antenna [8], were designed with FR-4 dielectric substrate are not suitable for 5G communication because of comparatively high loss tangent. Nowadays, substrates with low loss tangent are preferred for emerging technologies. A T-shaped MIMO antenna resonating in 26.83 - 33.13 GHz and 34.17 - 38.13 GHz with split-ring resonator (SRR) and defected ground structure (DGS) was designed with Rogers Duroid 5880 for vehicular communication applications [9]. Quasi-Yagi antenna with Rogers RT/Duroid 5880 substrate was used to obtain broadband as well as multi-band operations in 27.0 - 29.0 GHz and 36.0 - 40.0 GHz frequency bands [10]. Plexiglass substrate can be used to cover 23.92 - 43.80 GHz frequency band, having more than 87.45% efficiency in band [11].

Substrate-integrated waveguide (SIW) slot antenna with microstrip line feed having 2 dielectric layers and 3 copper layers was used to achieve 20.0 - 30.0 GHz wideband. This antenna was made using RT/Duroid 5880 LZ and provides 8.0 dBi gain [12]. Taylor n-bar amplitude taper with unequal power dividers attained 11.50 dBi gain in 27.50 - 28.65 GHz frequency band printed with Rogers RT/Duroid 5880 substrate [13]. Capacitively loaded loop (CLL) unit-cells covered 25.0 - 30.0 GHz band on Nelco NY 9220 substrate [14]. Two co-centric wire hexagons backed by another hexagonal ground loop fabricated on Rogers RT/Duroid 5880 substrate covered 25.05 - 34.92 GHz frequency band [15]. Beamforming network (BFN) covering 18.0 - 38.0 GHz frequency band, fabricated with liquid crystal polymer [16][17], fabry-perot resonant antenna covering 25.0 - 33.0 GHz band [18], and wideband microstrip comb-line linear array antenna covering 23.50 - 33.11 GHz [19] are used to attain high frequency response due to unique antenna structure.

Dielectric resonator antenna (DRA) fabricated with Rogers 5880 substrate, resonating between 27.25 - 28.59 GHz and produced 24.0 dB isolation [20]. A synthetic aperture radar (SAR) having 8 rotated slot antennas covered 27.20 - 28.20 GHz frequency band was used for 5G communication [21]. 5G with coplanar waveguide-fed (CPW) and T-shaped radiating patch element designed with Rogers RT Duroid 5880 substrate were used to achieve better frequency response between 25.1 - 37.5 GHz frequency band [22]. An omnidirectional antenna having radius and height equal to 0.19 mm and 0.15 mm respectively were used to achieve minimum 2.2 dBi gain using Rogers 6006 substrate in 26.5 - 28.7 GHz frequency band [23]. Techniques such as SIW corrugated printed with Rogers 5880 substrate in 26.8 - 28.4 GHz frequency

range [24], and enhanced central force optimization-Nelder-Mead (ECFO-NM) fabricated with Rogers Duroid RT 5880 substrate covering 28.0 - 38.0 GHz [25] were considered for better performance characteristics for 5G. For mobile phone circuit board, CP antenna with N9000 PTFE, covering frequency range of 27.0 - 40.0 GHz [26], and 28.0 GHz beam steering array on Rogers 5880 covering frequency range 27.5 - 30.0 GHz and having 16 cavity-backed slot antennas were designed [27] for 5G applications.

The mmw high gain antenna using RO 4003C and RO 5880 substrates resonated in 22.0 - 32.0 GHz [28], and CP-SIW antenna on Rogers 4350B resonated in 27.1 - 29.95 GHz (LHCP) and 26.55 - 29.55 GHz (RHCP) have better 5G performance characteristics [29]. MIMO antenna with dual band elimination characteristics [30], with identical dual-antenna building blocks (DABBs) [31], and for X-band satellite communication [32] were designed for 5G communication system.

Above discussed antennas have limited gain in comparatively high sizes and very high values of envelope correlation coefficients (ECCs). Also, these considered references have not discussed about the mean effective gain (MEG) for indoor and outdoor applications, and total active reflection coefficient (TARC) for excitation angles at ports and active bandwidth. At very high frequencies, effects of these parameters play a very important role in designing of high isolation, high gain, and high efficiency antennas.

In this paper, two port 50 Ω MIMO-array antenna with 2:1 VSWR impedance band is proposed to resonant at 28.0 GHz frequency. The designed antenna covers 27.04 - 28.35 GHz frequency band (1.31 GHz bandwidth) and more than 28.0 dB isolation between ports. Radiators at ports are uniquely arranged in parallel fashion, having 45^0 chopping at the corner patches to have very low return loss. The designed MIMO-array antenna provides greater than 13.99 dBi gain in presented frequency band.

2 MIMO Beamforming Antenna Design

The computer simulation tool microwave studio (CST MWS) is used for optimizing and designing the proposed structure. The initial design parameters are decided using particle swarm organization (PSO). A compact 2-port MIMO-array antenna on Rogers Duroid 5880 substrate with dielectric constant (r) = 2.2, loss tangent ($\tan(\delta)$) = 0.0009 is designed with full copper ground for the 5G application. The dielectric thickness of the substrate is 0.79 mm, while copper thickness is 0.035 mm. The 2×12 MIMO-array antenna is made on substrate dimension of 51.45×36.87 mm^2 The connectors with the proper frequency range are used at the ports. The used connectors have proper calibration before the measurements. The center to center separation

between two ports is 26.22 mm. This separation is required for the proper isolation between the radiating ports and for the maximization of the considered antenna performance parameters i.e. gain, efficiency, ECC, MEG, and TARC. This is done with the PSO optimization tool. For the proper tuning of the proposed MIMO-array antenna at the resonant frequency, electrical length is required. The electrical length (λ) for the designed MIMO-array antenna is 7.18 mm (this is corresponding to the length of the antenna equals 47.10 mm). Due to this the length of the antenna can be 6.57λ (using mm unit).

The widths of rectangular patches are according with 50 Ω feed lines at each port. To decrease the return loss at ports, patches situated at the edges are cut at the corners. Elements at each patch are connected with 50 Ω feed with the help of 70.7 Ω quarter wave line for better impedance matching and desired performance parameters. The CST optimized values are given in table 1. The schematic and fabricated views of designed MIMO antenna are given in figures 1 and 2 respectively.

Table 1 Optimized dimensions of proposed MIMO-array antenna (mm)

Parameter	l1	w1	l2	w2	l3	l4	w4	l5	w5	l6	w6	L	W
Value	3.56	2.43	3.23	0.37	1.36	2.70	3.267	3.67	4.23	3.56	2.43	51.45	36.87

3 Results and Discussion

The proposed MIMO-array antenna design is validated using vector network analyzer (VNA)-HP8720B and in anechoic chamber for S parameters and far-field results. The proposed MIMO-array antenna is designed in five steps. In first step, the single patch of 50 Ω feedline is selected. This antenna is unable to resonate in considered 5G band between 27.50 - 28.28 GHz. In second step, 50 Ω feed is combined with 70.7 Ω quarter wave line. The modified feedline decreases the size of proposed antenna implementation and also provides the impedance matching. Here, -6.0 dB return loss (VSWR = 3:1) band of 26.83 - 28.99 GHz is achieved. The bandwidth in this case is 2.16 GHz. In third step, corner-patches are chopped to improve return loss and are joined to 50 Ω feedline to other blocks of patches. Hence, three patches are connected to the single port. Antenna covers -6.0 dB return loss band of 27.55 - 28.51 GHz, where bandwidth is 960.0 MHz. In fourth step, three patches are transformed to four patches, all connected to single port. Here, antenna covers -6.0 dB return loss band of 28.526 29.344 GHz, having bandwidth of 818.33 MHz. In fifth step, antenna is converted to 8 patches with single port. With -10.0 dB return loss, antenna covers band of 28.52 29.467 GHz, having 946.54 MHz bandwidth.

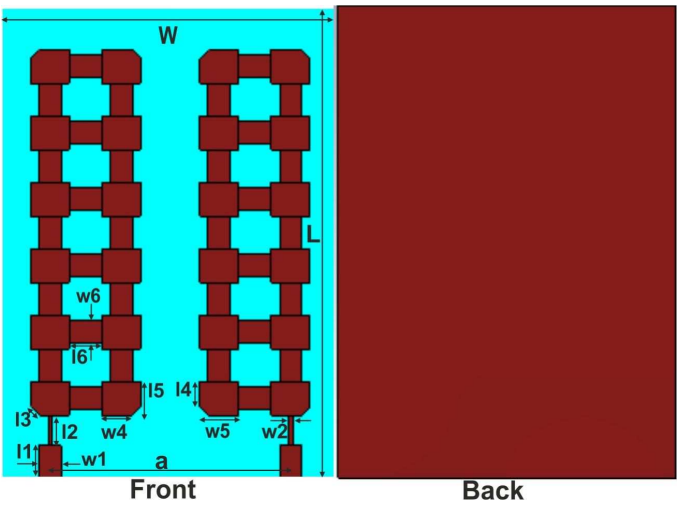

Fig. 1 Schematic views of proposed MIMO-array antenna

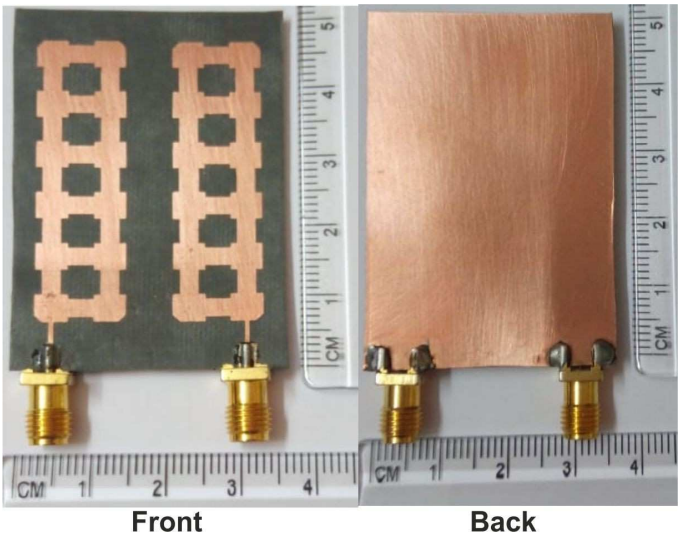

Fig. 2 Fabricated views of proposed MIMO-array antenna

In sixth step, antenna is connected to 12 patches to single port and is the proposed structure to resonate at 28.0 GHz frequency. The considered single port antenna covers -10.0 dB return loss band of 27.10 - 28.33 GHz, and provides 1.23 GHz bandwidth. Finally, seventh step is the proposed MIMO-array antenna. In this case, MIMO-array covers -10.0 dB return loss band of 27.04 - 28.35 GHz, and provides 1.31 GHz bandwidth. All the design steps are shown in figure 3, and their return loss parameters (S_{11}) are compared in figure 4 respectively.

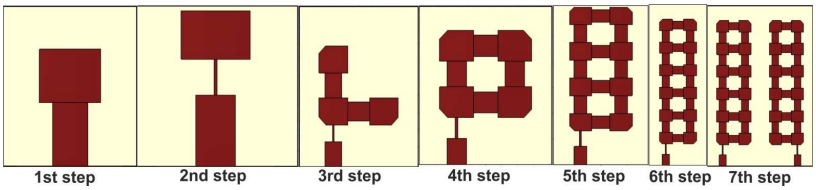

Fig. 3 Design steps of proposed MIMO-array antenna

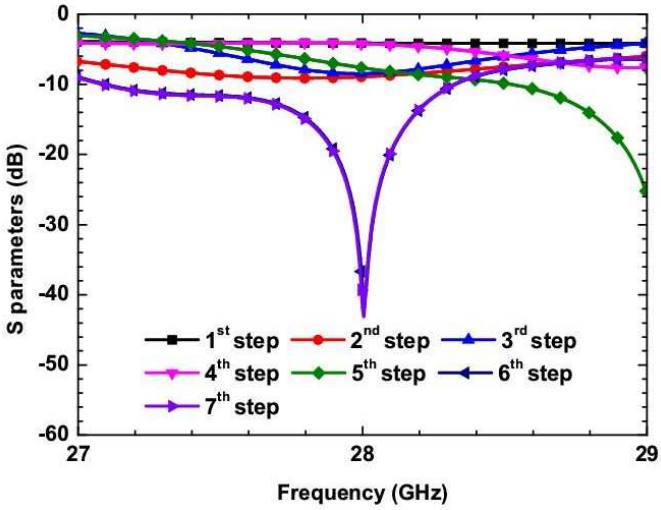

Fig. 4 S_{11} parameter of design steps

The simulated results of single element with different stages have been discussed above. The single element with 2:1 VSWR resonates in 27.06 - 28.35 GHz band and provides 1.29 GHz bandwidth, while 2-port MIMO-array covers 2:1 VSWR band of 27.04 - 28.35 GHz and provides 1.31 GHz bandwidth. Slight increase in MIMO bandwidth shows that MIMO has better performance than single element. The measured 2:1 VSWR band of 27.06 - 28.54 GHz is obtained using VNA. The measured bandwidth is 1.48 GHz. The difference in simulated and measured bandwidths is due to the port coupling losses and fabrication errors. The simulated and measured results are compared in figure 5. As gain is inversely proportional to bandwidth, therefore simulated gain of SISO is 16.07 dBi while that of MIMO is 15.46 dBi at 28.0 GHz. Due to simplicity, only S_{11} and S_{12} parameters are considered in this paper (because $S_{11} = S_{22}$ and $S_{12} = S_{21}$).

The effect of mutual coupling or isolation between the radiating ports can be studied in terms of surface current distribution. Surface current distribution at each port can be obtained by exciting any one port at a time and vice versa of proposed antenna. For this, port 1 is excited and other port is terminated by 50 Ω impedance to observe the effect of current distribution. Each patch

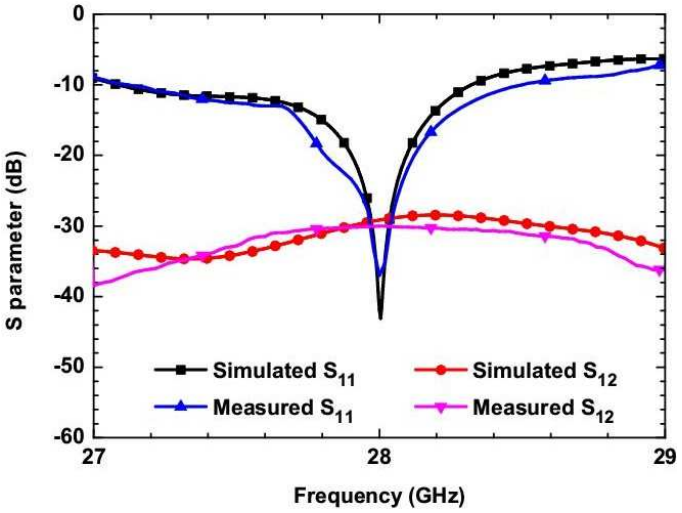

Fig. 5 S-parameters of proposed MIMO-array antenna

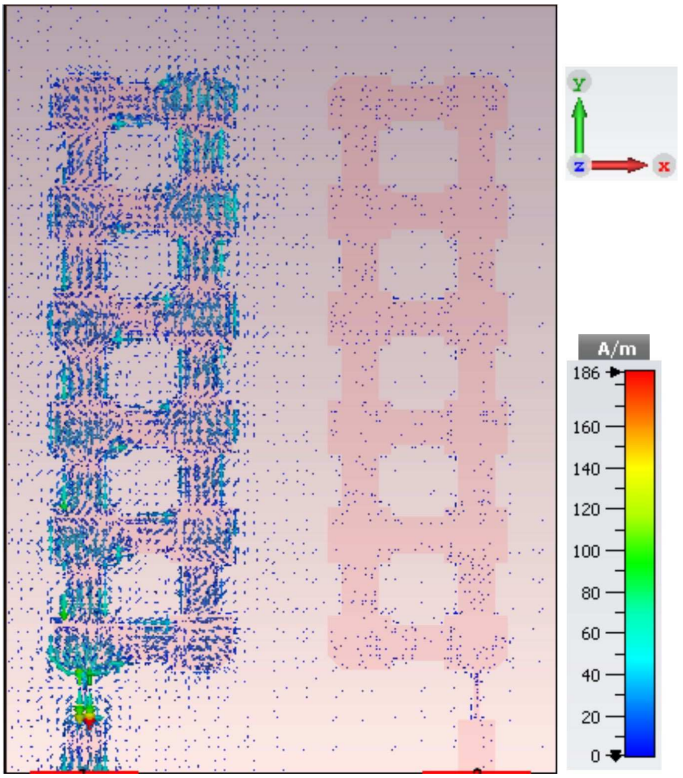

Fig. 6 Surface current distribution of MIMO-array antenna at port 1

antenna gets the power from the lower patch antenna via feed arm. The red arrow is the representation of the maximum current concentrated on the feed arm and the different colored arrows represent the varying amount of current on upper sides of the antenna patches and feed arms. As shown in figure 6, maximum current is concentrated at the joint point of 50 Ω and 70.7 Ω transmission lines. The simulated range of current at 28.0 GHz resonant frequency is 0 - 186 A/m. The high current range is due to the operation of the proposed MIMO-array antenna at 28.0 GHz frequency. Except the joint point, very low value of current is observed at other radiating port. Due to the concentration of different amount of currents on different parts of the antenna at port 1, less current is linked to the antenna at port 2. This is one of the reasons to provide better than 28.0 dB isolation at ports. The result of port 1 is shown only. Due to the symmetric structure, same results are observed at port 2.

The parametric sweep for the proposed MIMO-array antenna is carried out to observe the tuning effect of it with the variation in length and width of the critical parameters. A parametric sweep has been carried out to observe effects on S-parameters by varying length of transmission line (l6) in the range of 1.56 - 5.56 mm. The width of transmission line (w6) is fixed at 2.43 mm. The length of transmission line changes the electrical length of the proposed antenna. As can be seen from figure 7, other than the selected length = 3.56 mm, antenna is unable to resonate below -10.0 dB for lower values of length, and for higher values, it is resonating at around 27.0 GHz and 29.0 GHz frequencies, having very high return losses. It is observed that return loss parameter S_{11} shows major changes in its values, and there are only minor variations in isolation parameter S_{12}.

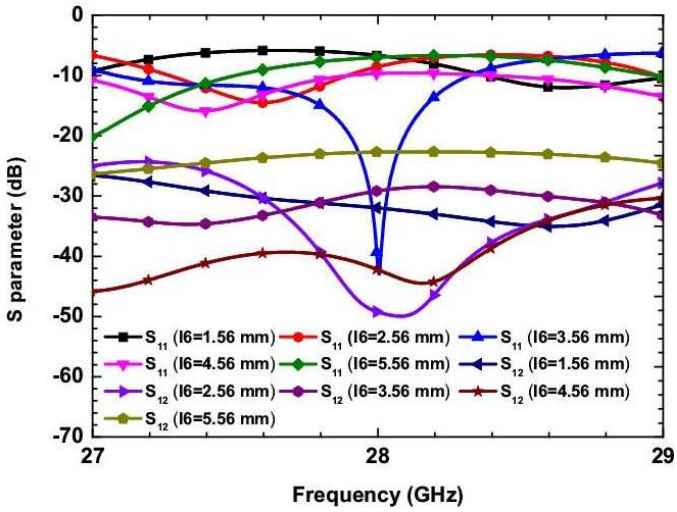

Fig. 7 Effect of transmission line length (l6) on S-parameter

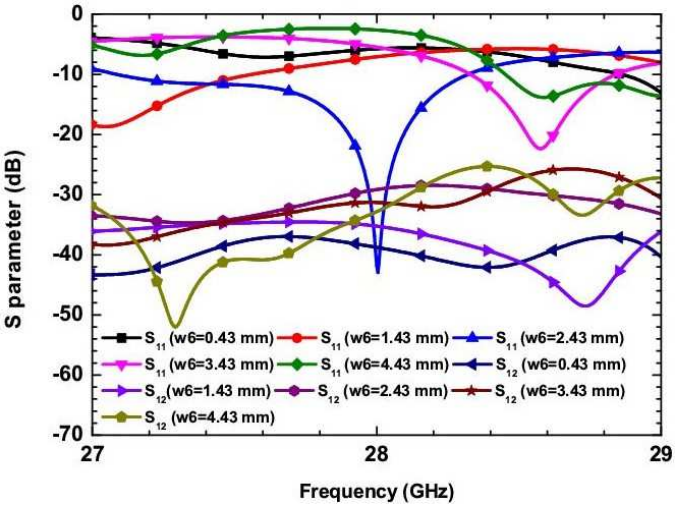

Fig. 8 Effect of transmission line width (w6) on S-parameter

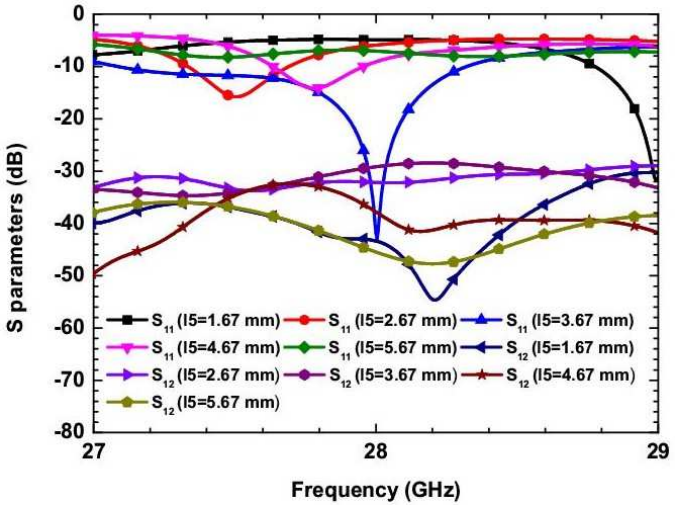

Fig. 9 Effect of length of patch (l5) on S-parameter

As shown in figure 8, when width of transmission line (w6) is varied between 0.43 - 4.43 mm, multiple bands are obtained at different frequencies with high return losses. The width of transmission line is responsible for changing the impedance of the antenna. More than -40.0 dB return loss is observed at selected value of w6 = 2.43 mm. The length l6 is fixed at 3.56 mm. Not much difference is obtained in isolation parameter S_{12}.

The variation in length of patch (l5) from 1.67 - 5.67 mm is observed in figure 9. The width w5 is fixed at 4.23 mm. The length of patch is fixed

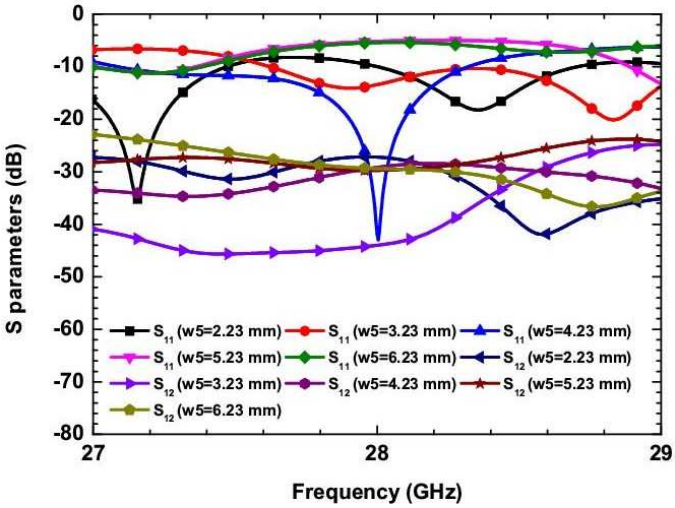

Fig. 10 Effect of width of patch (w5) on S-parameter

at 3.67 mm. Single or multiple bands are obtained at other than 28.0 GHz frequency with high return losses as compared to considered length of patch. No major changes are observed in isolation parameter S_{12}.

Similarly, from figure 10, effects on S_{11} are observed by varying width of patch (w5) from 2.23 - 6.23 mm. The length of patch is fixed at 3.67 mm. Other than considered value of w5 = 4.23 mm, antenna is resonating at different frequencies, generating multiple bands with high return losses. The minor variations are observed in isolation parameter S_{12}.

The diversity parameters ECC, MEG, and TARC are analyzed here for the effectiveness of the proposed MIMO-array structure. The ECC includes all ports and their return-losses and isolation parameters of the designed MIMO-array antenna and can also be obtained in terms of the far field radiation patterns. Formula of ECC (ρ_e) is given in equation 1 using far field patterns [33]. Simulated value of ECC lies in the range $\leqslant 10^{-4}$, which is very much lesser than the ECC value specified by ITU. The measured values of ECC using both the S-parameters and radiation patterns lie also in the range $\leqslant 10^{-4}$. Due to $\leqslant 10^{-4}$ ECC values, it looks close to zero values on x-axis. ECC also shows the proper correlation/isolation/coupling between radiating ports. A comparison between the simulated and measured ECC is shown in figure 11. Only minute changes are observed in simulated and measured ECC in the presented band. Very low values of ECCs in the whole band are one of the major advantages of the proposed MIMO-array antenna.

$$\rho_e = \frac{\int\int \bar{F}_1 . \bar{F}_2^* d\Omega^2}{\int\int \bar{F}_1{}^2 d\Omega . \int\int \bar{F}_2^2 d\Omega} \tag{1}$$

where, F_1 and F_2 are far-field patterns of antenna 1 and antenna 2 respectively and Ω is the solid angle.

Another diversity parameter MEG is analyzed here for the applicability of the proposed MIMO-array design for indoor and outdoor environments. The proposed design is cross checked for isotropic environment with cross-polarization ratio (XPR) = 0 dB and 6.0 dB, and for Gaussian environment with XPR = 0 dB and 6.0 dB respectively [33][34]. The value of XPR equals 0 dB for outdoor environment, and XPR equals 6.0 dB for indoor environment respectively are considered. A comparison among all the MEG values with different environments with different XPR values is shown in figure 12.

Formulas of the MEGs are given by equations 2 and 3 respectively:

$$MEG_j = \oint \left(\frac{XPR}{1+XPR} P_{\theta j(\Omega)} G_{\theta j(\Omega)} + \frac{1}{1+XPR} P_{\phi j(\Omega)} G_{\phi j(\Omega)} \right), \quad (2)$$

$$MEG_j = \frac{1}{2\pi} \int_0^{2\pi} \left[\frac{XPR}{1+XPR} G_{\theta j} \left(\frac{\pi}{2}, \phi \right) + \frac{1}{1+XPR} G_{\phi j} \left(\frac{\pi}{2}, \phi \right) \right] d\phi, \quad (3)$$

where, $G_{\theta j}$ and $G_{\phi j}$ are the gain parameters in azimuthal and elevation planes, $P_{\theta j}$ and $P_{\phi j}$ are the probability distribution functions in azimuthal and elevation planes respectively.

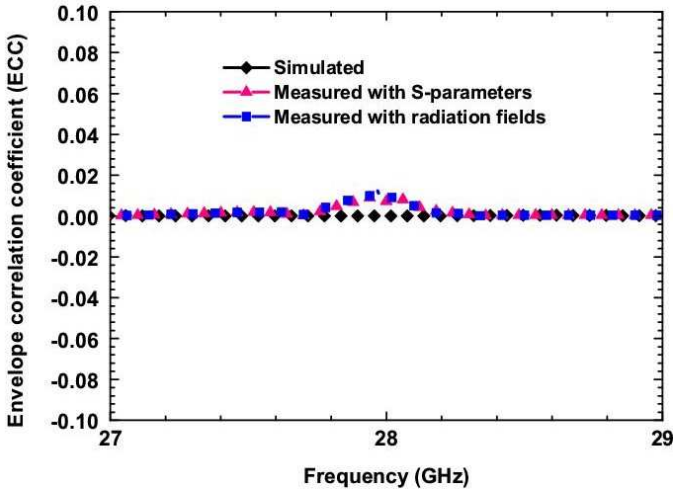

Fig. 11 ECC of proposed MIMO-array antenna

It is observed that, for isotropic environment with XPR = 6.0 dB, values of MEG are slightly greater than -3.0 dB, although for XPR = 0 dB its value is

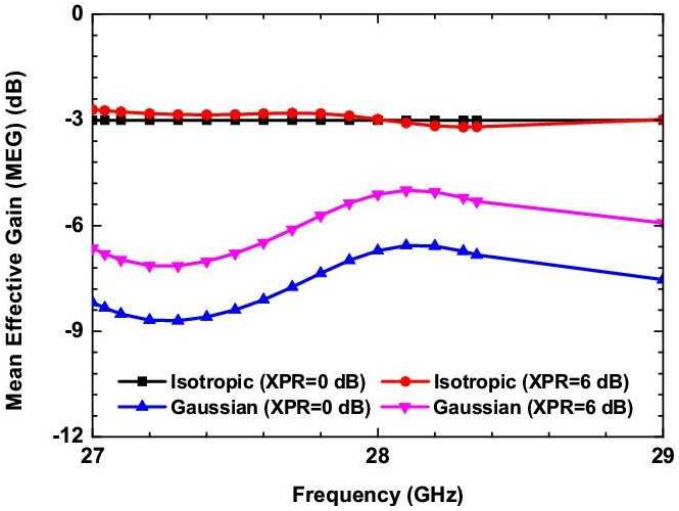

Fig. 12 MEG of proposed MIMO-array antenna

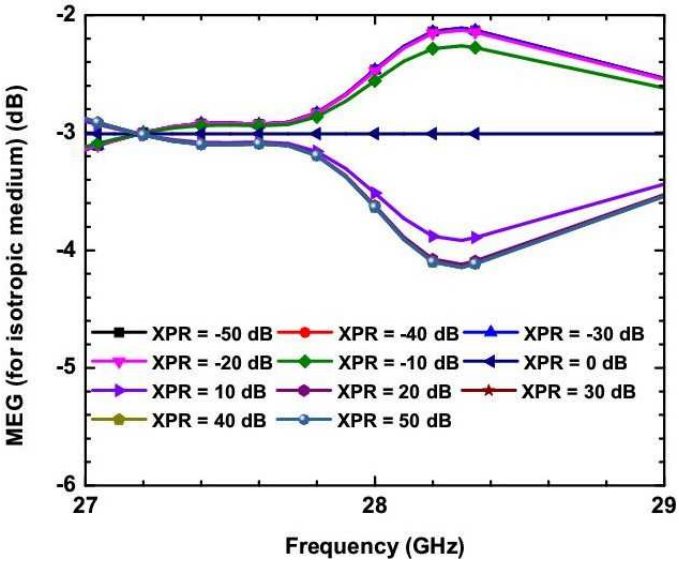

Fig. 13 MEG of proposed MIMO-array antenna for isotropic medium

around -3.0 dB. Therefore, proposed MIMO-array antenna shows its suitability for outdoor environment only, and is not suitable for indoor environment. Similarly, for Gaussian environment with XPR = 0 dB and 6.0 dB, MEG values are lesser than -5.0 dB. Therefore, proposed antenna shows the suitability for indoor as well as for outdoor environments. Hence, proposed MIMO-array antenna shows its strong candidature for Gaussian environment conditions.

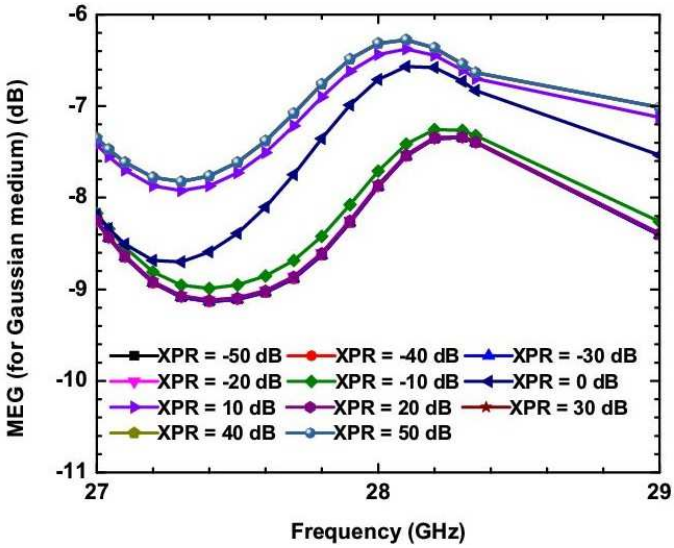

Fig. 14 MEG of proposed MIMO-array antenna for Gaussian medium

Now, a variation in XPR is also carried out to show the extension in the values of MEG. Figure 13 and 14 , show the variation in MEG for both the isotropic and Gaussian mediums with respect to the XPR values varying in the range -50.0 dB to 50.0 dB. For isotropic medium, when XPR $<$ 0 dB, MEG is slightly greater than -3.0 dB, while the rest values are lower than -3.0 dB in the considered 27.04 - 27.3 GHz frequency band. At XPR = 0 dB, its value is constant at -3.0 dB for the whole frequency band. Similarly when XPR $>$ 0 dB, MEG is slightly lower than -3.0 dB in 27.04 - 27.17 GHz band, while the rest values are greater than -3.0 dB for the remaining band. Similarly, for Gaussian medium, when XPR $<$ 0 dB, MEG values are lesser than -7.0 dB for the whole band. At XPR = 0 dB, MEG values are lower than -6.0 dB, while for XPR $>$ 0 dB, its value is lower than -6.0 dB. A favorable figure of merit is obtained in terms of the MEG diversity parameter for validation of indoor and outdoor environmental conditions.

Another diversity parameter TARC (Γ_a^t) is used to relate total incident power to total outgoing power for MIMO-array antennas. It is obtained using equation 4 [34]. The analysis of TARC is carried out in two steps. In first step, different angles of excitations at different ports are selected to find the variation in TARC. In second step, same excitation angles are selected at both the ports. It has been observed from figures 15 and 16 that, best combination of excitation angles 45^0, 45^0 produces relevant TARC responses for different excitation angles. Similarly, 0^0 excitation angle produces relevant TARC responses for same excitation angles at ports. Both the responses of TARC produce responses similarly to return loss S_{11}, and each TARC response curve shows its resonant around 28.0 GHz with small variations from resonant frequency.

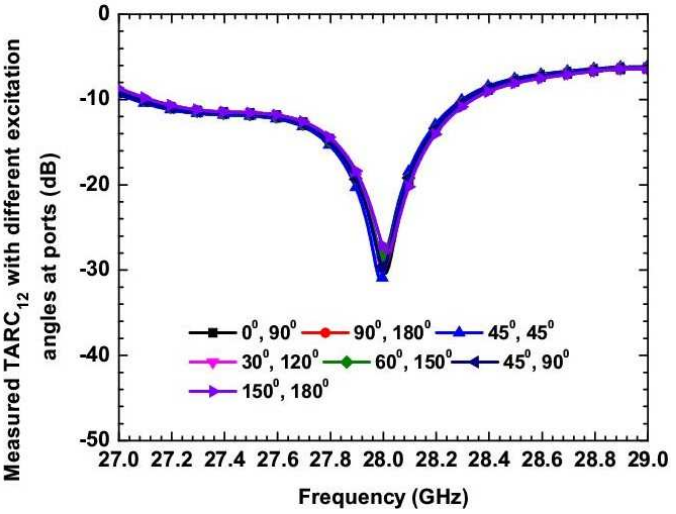

Fig. 15 TARC with different excitation angles at ports

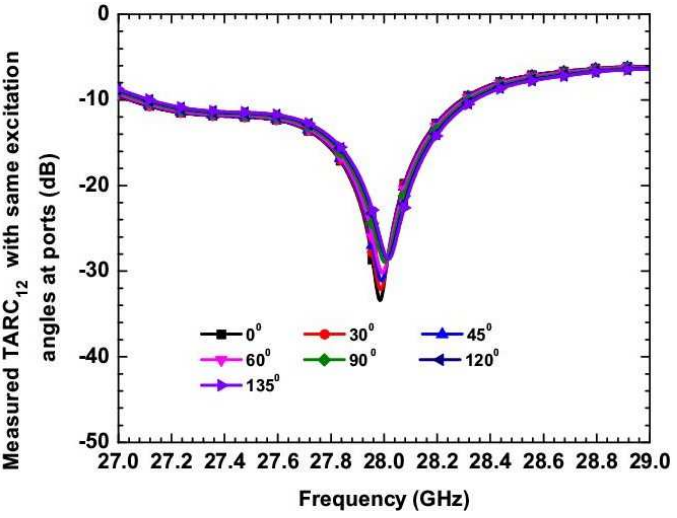

Fig. 16 TARC with same excitation angles at ports

The active TARC bandwidth in both the cases is approximately 1.3 GHz.

$$\Gamma_a^t = \frac{\sqrt{\left(S_{ii} + S_{ij} * e^{jq}\right)^2 + \left(S_{ji} + S_{jj} * e^{jq}\right)^2}}{\sqrt{N}}, \tag{4}$$

where, S_{ii} and S_{jj} are the return loss and isolation parameters at ports 1 and 2, and q is the input excitation angle.

The gain of the proposed MIMO-array antenna is measured in an anechoic chamber using E-field, in presence of standard horn antennas and microwave generator suitable to cover the presented band. The simulated and measured gains in the presented band are achieved between 13.99 - 15.46 dBi for the two ports, and are 15.03 - 16.07 dBi for single port. Slightly higher value of gain is obvious, as bandwidth is slightly lower in single element. This is the main reason that the gain is slightly lower in MIMO antennas as compared to single element. The FRIIS equation is used to find the gain after the measurement of the received power in anechoic chamber, and is given by equation 5 [33].

$$P_r = \frac{P_t G_t G_r \lambda^2}{(4\pi R)^2} \tag{5}$$

where, P_r is the received power by proposed array antenna, P_t is the transmitted power by the standard horn antenna, G_t is the gain of the transmitting horn antenna, G_r is gain of the receiving antenna, λ is wavelength, and R is distance between the antennas.

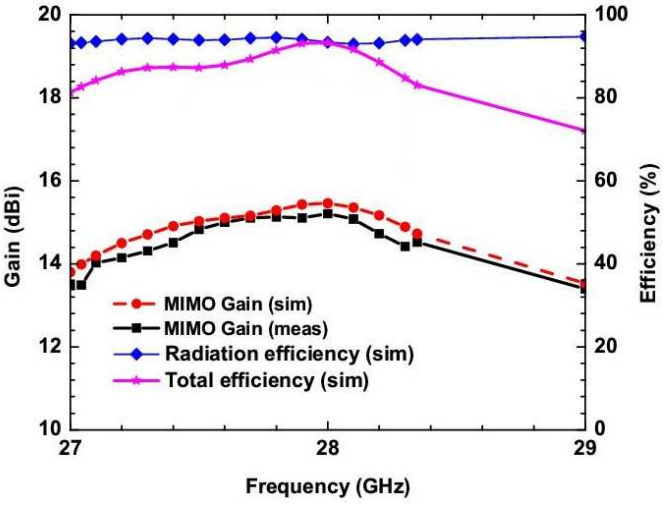

Fig. 17 Gain and efficiency of proposed MIMO-array antenna

The simulated radiation efficiency in the presented band lies in the range of 93.3% - 94.56%, and the simulated total efficiency lies in the range 82.69% - 93.3%. At 28.0 GHz resonant frequency, simulated and measured gains are 15.46 dBi and 15.21 dBi, and simulated radiation efficiency is 93.43%. The overall efficiency is calculated as per given in equation 6. The reason of high radiation efficiency is due to the lower losses and high impedance matching.

$$e_0 = e_r e_c e_d \tag{6}$$

where, e_0 is total efficiency, e_r is reflection (mismatch) efficiency, e_c is conduction efficiency, and e_d is dielectric efficiency.

The product of e_c and e_d is known as the radiation efficiency. All the gains and efficiencies are compared in figure 17. The directivity (D) of the proposed array antenna can be obtained using the formula given in equation 7 [33].

$$D = \frac{41253}{(\theta_E \theta_H)}, \tag{7}$$

where, θ_E is the half power beamwidth in E-plane, and is the half power beamwidth θ_H in H-plane of the proposed array antenna.

Table 2 Comparison of proposed MIMO-array antenna design with existing designs

Reference	Substrate	Dimension	Gain	Efficiency	ECC	No. of elements	No. of ports	Isolation	Frequency band
[2]	Rogers 5880	135 × 75 mm^2	10 dBi	-	<0.015	-	8	> 14.52 dB	27.5 - 31.0 GHz
[4]	Rogers 5880	30 × 43 mm^2	10.27 dBi	-	<0.1 10^{-6}	-	4	> -45 dB	24.5 - 26.5 GHz
[7]	Rogers RT Duroid 5880	12.0 × 25.4 × 0.8 mm^3	7.11 dBi	-	<0.5	2	2	-	26.83 - 33.13 GHz, 34.17 - 38.13 GHz
[8]	Rogers RT/ Duroid 5880	20.0 × 23.0 mm^2	10.5 dBi	-	-	16	1	-	27.0 - 29.0 GHz, 36.0 - 40.0 GHz (multi) and 24.8 - 40.0 GHz (broad)
[10]	RT/ Duroid 5880 LZ	34.95 mm^2, 35.72 mm^2	8.0 dBi	-	-	-	1	-	20.0 - 30.0 GHz
[11]	Rogers RT Duroid 5880	40.0 × 50.0 mm^2	11.5 dBi	66.0%	-	8	1	-	27.5 - 28.65 GHz
[13]	Rogers RT/ Duroid 5880	40.0 × 20.0 mm^2	12.15 dBi	85.0%	-	1	1	-	25.05 - 34.92 GHz
[16]	Rogers RO 5880	17.064 × 17.064 × 7.56 mm^3	14.1 dBi	-	-	4	4	>25.0 dB	25.0 - 33.0 GHz
[18]	Rogers 5880	20.0 × 20.0 mm^2	8.0 - 10.0 dBi	-	<0.013	2	2	24.0 dB	27.25 - 28.59 GHz
[20]	Rogers RT Duroid 5880	12.0 × 12.0 mm^2	10.6 dBi	>80.0%	⩽ 0.009	4	4	-	25.1 - 37.5 GHz
[22]	Rogers 5880	72.0 × 17.2 mm^2, 39.8 × 33.4 mm^2	9.5 dBi, 11.0 dBi	-	< 0.002	4	4	<20.0 dB	26.8 - 28.4 GHz
[25]	Rogers 5880	5.8 × 1.5 mm^2	6.9 dBi	-	-	8	8	> 17.0 dB	27.5 - 30.0 GHz
Proposed work	Rogers RT 5880	51.44 × 36.87 mm^2	15.46 dBi	> 93.0%	⩽ 10^{-4}	24	2	> 28.0 dB	27.04 - 28.35 GHz

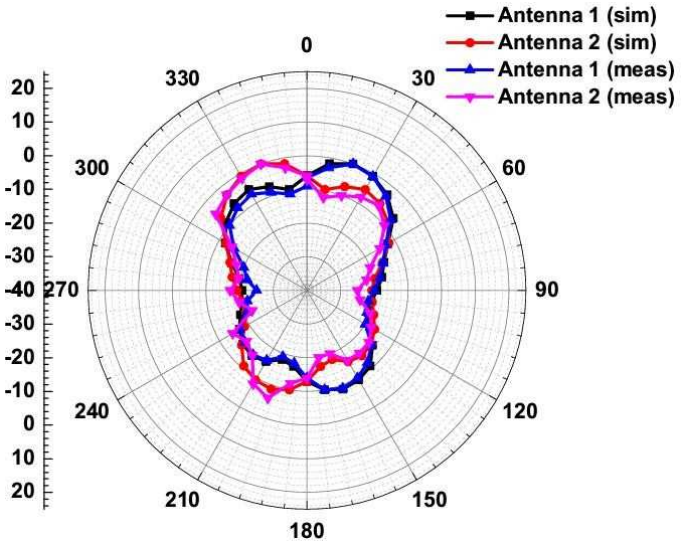

Fig. 18 E-field radiation patterns of proposed MIMO-array antenna

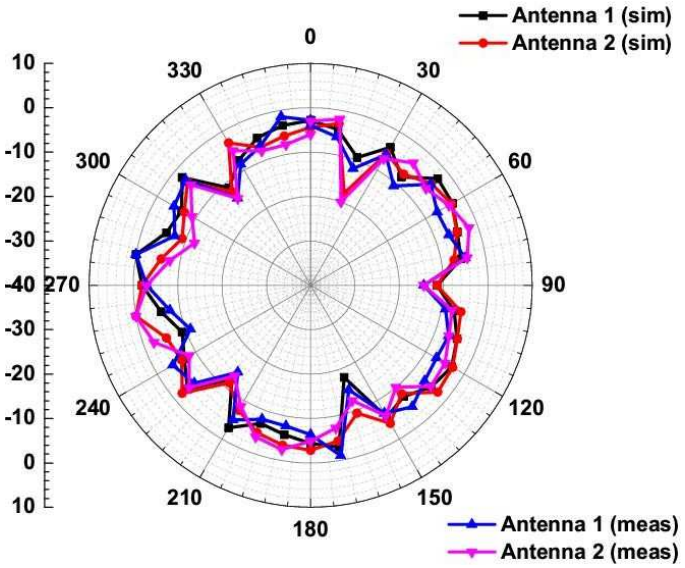

Fig. 19 H-field radiation patterns of proposed MIMO-array antenna

4 Conclusion

A 2-port MIMO-array antenna has been proposed for 5G applications to work for millimeter-wave frequency band. With 2:1 VSWR, proposed antenna resonated at 28.0 GHz and covered 27.04 - 28.35 GHz frequency band. The design exhibited more than 28.0 dB isolation between ports, more than 93.0%

radiation efficiency, and 13.99 dBi minimum gain in whole frequency band. At 28.0 GHz resonant frequency, obtained gain is 15.46 dBi. The ECC in the presented band is $\leq 10^{-4}$, which is one of the most important aspects of the designed prototype. The design showed its applicability in indoor and outdoor Gaussian applications completely, and has 1.31 GHz TARC active bandwidth.

5 Declarations

The paper has original contribution of the research work done for the 5G MIMO-array antenna design.

5.1 Funding

There is no funding received from any source for this research.

5.2 Conflicts of interest/Competing interests

The authors have the original work for the 5G MIMO-array antenna design. There is no conflict of this work with any other author or research.

5.3 Availability of data and material

There is no data or material is available separately.

5.4 Code availability

None

5.5 Authors' contributions

All the authors names included in author list have equally contributed in research work.

References

[1] Kachhavay, M.G. and Thakare, A.P. (2014). 5G Technology- Evolution and Revolution. International Journal of Computer Science and Mobile Computing 3, 1080-1087.

[2] Shaza, M.El-Nady, and Ahmed, M. Attiya., (2022). Periodically-stub loaded Microstrip line Wideband circularly polarized Millimeter wave MIMO antenna. IEEE Access., 10, 20465-20472.

[3] Arpan, D., Cong Danh, B., Jay, P. Trushit, U., Gangil, B., Truong Khan, N., (2020). Compact wideband four element Optically transparent MIMO antenna for mm-wave 5G Applications. IEEE Access., 8, 194206-194217.

[4] Saba, T., Syeda, I.N., Niamat, H., (2021). A metasurface-based MIMO antenna for 5G millinete-wave applications. IEEE Access., 9, 51805-51817.

[5] Bhat, I.N. and Dogra, H. (2016). Beamforming in 5G Networks. International Journal of Trend in Scientific Research and Development 2, 39-42.

[6] Malviya, L., Kartikeyan, M.V., Panigrahi, R.K. (2018). Multi-standard, multi-band planar multiple input multiple output antenna with diversity effects for wireless applications. Int J RF Microw Comput Aided Eng,29(2), 1-8.

[7] Malviya, L., Panigrahi, R.K., Kartikeyan, M.V., (2017). A low profile planar MIMO antenna with polarization diversity for LTE 1800/1900 applications. Microw Opt Technol Lett., 59(3), 533-538.

[8] Malviya, L., Panigrahi, R.K., Kartikeyan, M.V., (2018). Offset planar MIMO antenna for omnidirectional radiation patterns. Int J RF Microw Comput Aided Eng., 28(6), 1-9.

[9] Venkateswara, R.M., Madhav, B.T.P., Krishna, J., Usha, D.Y., Anilkumar, T., Prudhvi, N.B.,(2019). CSRR-loaded T-shaped MIMO antenna for 5G cellular networks and vehicular communications. Int J RF Microw Comput Aided Eng., 29(8), 1-14.

[10] Nouri, M., Aghdam, S.A., Jafarieh, A., Bagby, J., Sahebghalam, S.,(2019). A wideband millimeter-wave antenna based on quasiYagi antenna with MIMO circular array antenna beamforming for 5G wireless networks. Microw Opt Technol Lett., 61(7), 1810-1814.

[11] Desai, A., Upadhyaya, T., Patel, R., (2019). Compact wideband transparent antenna for 5G communication systems. Microw Opt Technol Lett., 61(3), 781-786.

[12] Di Renna, R.B., Magri Souza, V.P.R., Ferreira, T.N., Matos, L.J., Souza, J.A.M., Siqueira GL., (2019). A new double-sided substrate-integrated waveguide slot array antenna for 5G applications. Microw Opt Technol Lett., 61(3), 682-687.

[13] Hill, T.A., Kelly, J.R., (2019). 28 GHz Taylor feed network for sidelobe level reduction in 5G phased array antennas. Microw Opt Technol Lett, 61(1), 37-43.

[14] Wani, Z., Abegaonkar, M.P., Koul, S.K., (2018). Millimeter-wave antenna with wide-scan angle radiation characteristics for MIMO applications. Int J RF Microw Comput Aided Eng., 29(5), 1-9.

[15] Ullah, H., Tahir, F.A., (2019). A broadband wire hexagon antenna array for future 5G communications in 28 GHz band. Microw Opt Technol Lett., 61(3), 696-701.

[16] Rahimian, A., Abbasi, Q.H., Alomainy, A., Alfadhl, Y., (2019). A low-profile 28-GHz Rotman lens-fed array beamformer for 5G conformal subsystems. Microw Opt Technol Lett., 61(3):671-675.

[17] Mujammami, E.H., Afifi, I., Sebak, A., (2019). Optimum wideband high gain analog beamforming network for 5G applications. IEEE Access., 7, 52226-52237.

[18] Hussain, N., Jeong, M.J., Kim, N., (2019). A broadband circularly polarized fabry-perot resonant antenna using a single-layered PRS for 5G MIMO applications. IEEE Access., 7, 42897-42907.

[19] Afoakwa, S., Jung, Y.B., (2017). Wideband microstrip comb-line linear array antenna using stubbed-element technique for high sidelobe suppression. IEEE Transactions on antennas and propagation., 65(10), 5190-5199.

[20] Zhang, Y., Deng, J.Y., Li, M.J., Sun, D., Guo, L.X., (2019). A MIMO dielectric resonator antenna with improved isolation for 5G mm-wave applications. IEEE Antennas and wireless propagation letters., 18(4), 747-751.

[21] Bang, J., Choi, J., (2018). A SAR reduced mm-wave beam-steerable array antenna with dual-mode operation for fully metal- covered 5G cellular handsets. IEEE Antennas and wireless propagation letters., 17(6), 1118-1122.

[22] Jilani, S.F., Alomainy, A., (2018). Millimetre-wave T-shaped MIMO antenna with defected ground structures for 5G cellular networks. IET Microwaves, Antennas and propagation., 12(5), 672-677.

[23] Lin, W., Ziolkowski, R.W., Baum, T.C., (2017). 28 GHz compact omnidirectional circularly polarized antenna for device-to-device communications in the future 5G systems. IEEE Transactions on antennas and propagation., 65(12), 6904-6914.

[24] Lin, M., Liu, P., Guo, Z., (2017). Gain-enhanced Ka-band MIMO antennas based on the SIW corrugated technique. IEEE Antennas and wireless propagation letters., 16, 3084-3087.

[25] Mahmoud, K.R., Montaser, A.M., (2017). Optimised 4 x 4 millimetre-wave antenna array with DGS using hybrid ECFO-NM algorithm for 5G mobile networks. IET Microwaves, antennas and propagation., 11(11),

1516-1523.

[26] Mahmoud, K.R., Montaser, A.M., (2017). Design of dual-band circularly polarised array antenna package for 5G mobile terminals with beam-steering capabilities. IET Microwaves, antennas and propagation., 12(1), 29-39.

[27] Yu, B., Yang, K., Sim, C.Y.D., Yang, G., (2018). A novel 28 GHz beam steering array for 5G mobile device with metallic casing application. IEEE Transactions on antennas and propagation., 66(1), 462-466.

[28] Mao, C.X., Gao, S., Wang, Y., (2017). Broadband high-gain beam-scanning antenna array for millimeter-wave applications. IEEE Transactions on antennas and propagation., 65(9), 4864-4868.

[29] Park, S.J., Park, S.O., (2016). LHCP and RHCP substrate-integrated-waveguide antenna arrays for millimeter-wave applications. IEEE Antennas and wireless propagation letters., 16, 601-604.

[30] Raheja, D.K., Kanaujia, B.K., Kumar, S., (2019). Compact four-port MIMO antenna on slotted-edge substrate with dual-band rejection characteristics. Int J RF Microw Comput Aided Eng., 29(7), 1-10.

[31] Zou, H., Li, Y., Xu, B., Luo, Y., Wang, M., Yang, G., (2019). A dual-band eight-antenna multi-input multi-output array for 5G metal-framed smartphones. Int J RF Microw Comput Aided Eng., 29(7), 1-15.

[32] Sharma, N., Bhatia, S.S., (2019). Design of printed monopole antenna with band notch characteristics for ultra-wideband applications. Int J RF Microw Comput Aided Eng., 29(10), 1-18.

[33] Malviya, L., Panigrahi, R.K., Kartikeyan, M.V., (2017). MIMO antennas with diversity and mutual coupling reduction tech- niques: a review. Int J of Microw. and Wireless Technologies., 9(8), 1763-1780.

[34] Gupta, P., Malviya, L., Charhate, S.V., (2019). 5G multi-element/port antenna design for wireless applications: a review. Int J of Microw. and Wireless Technologies., 11(9), 918-938.